BRAIN
ORIGINAL ARTICLE

# Pre-ataxic loss of intrinsic plasticity and motor learning in a mouse model of SCA1

Catarina Osório,† Joshua J. White,† Heiling Lu, Gerrit C. Beekhof, Francesca Romana Fiocchi, Charlotte A. Andriessen, Stephanie Dijkhuizen, Laura Post and Martijn Schonewille

†These authors contributed equally to this work.

Spinocerebellar ataxias are neurodegenerative diseases, the hallmark symptom of which is the development of ataxia due to cerebellar dysfunction. Purkinje cells, the principal neurons of the cerebellar cortex, are the main cells affected in these disorders, but the sequence of pathological events leading to their dysfunction is poorly understood. Understanding the origins of Purkinje cells dysfunction before it manifests is imperative to interpret the functional and behavioural consequences of cerebellar-related disorders, providing an optimal timeline for therapeutic interventions.

Here, we report the cascade of events leading to Purkinje cells dysfunction before the onset of ataxia in a mouse model of spinocerebellar ataxia 1 (SCA1). Spatiotemporal characterization of the ATXN1[82Q] SCA1 mouse model revealed high levels of the mutant ATXN1[82Q] weeks before the onset of ataxia. The expression of the toxic protein first caused a reduction of Purkinje cells intrinsic excitability, which was followed by atrophy of Purkinje cells dendrite arborization and aberrant glutamatergic signalling, finally leading to disruption of Purkinje cells innervation of climbing fibres and loss of intrinsic plasticity of Purkinje cells. Functionally, we found that deficits in eyeblink conditioning, a form of cerebellum-dependent motor learning, precede the onset of ataxia, matching the timeline of climbing fibre degeneration and reduced intrinsic plasticity.

Together, our results suggest that abnormal synaptic signalling and intrinsic plasticity during the pre-ataxia stage of spinocerebellar ataxias underlie an aberrant cerebellar circuitry that anticipates the full extent of the disease severity. Furthermore, our work indicates the potential for eyeblink conditioning to be used as a sensitive tool to detect early cerebellar dysfunction as a sign of future disease.

Department of Neuroscience, Erasmus Medical Center, Rotterdam 3015CN, The Netherlands

Correspondence to: Martijn Schonewille
Department of Neuroscience
Erasmus Medical Center
Rotterdam 3015CN, The Netherlands
E-mail: m.schonewille@erasmusmc.nl

Keywords: cerebellum; purkinje cell; eyeblink conditioning; presymptomatic; ataxin1

Received April 16, 2022. Revised October 04, 2022. Accepted October 24, 2022. Advance access publication November 10, 2022

## Introduction

Spinocerebellar ataxias (SCAs) are a group of autosomal-dominant, inherited neurodegenerative disorders, characterized by a progressive loss of balance and motor coordination.[1,2] The onset of ataxia, the lack of muscle control or coordination of voluntary movements, is the first clinical manifestation in SCA patients derived from cerebellar and brainstem dysfunction.[3] However, a growing body of evidence shows that early pathological changes are identifiable during the preclinical stage. Longitudinal studies have revealed that asymptomatic carriers of SCA1 and SCA2 mutations had mild coordination deficits as well as grey matter loss in the cerebellum and brainstem years before the appearance of ataxia symptoms.[4-6] Preclinical dysfunction in saccades was identified in asymptomatic carriers of SCA3 and SCA7 mutations.[7,8] Similar pre-ataxic deficits were observed when eyeblink conditioning (EBC), a classical cerebellum-dependent learning task, was tested in asymptomatic carriers of SCA3.[9] Indeed, experiments in a mouse model of SCA1 demonstrated that the delay of the expression of the mutant ATXN1 until after the pre-ataxia period decreased the severity of disease.[10] Evidence from mouse studies supports the potential for antisense oligonucleotide therapy to rescue SCAs,[11] but the clinical application is currently primarily focused on disorders with a clear early onset and clear timeline of disease progression.[12-15] These data suggest that the study of the preclinical or pre-ataxia stage is of great importance for a better understanding of disease aetiology and progression, while revealing an optimal time window for therapeutic interventions.

Regardless of the genetic heterogeneity in the different SCAs, Purkinje cell (PC) dysfunction and/or degeneration is a common pathogenic mechanism underlying motor deficits.[16,17] PCs are the core processing units of the cerebellar cortex[18,19] critical for motor control,[20,21] motor learning[22,23] and non-motor functions such cognition[24] and emotion.[25] With this variety of functions, there is no surprise that small alterations in their cytoarchitecture or activity are sufficient to compromise brain function. Changes in transcriptional regulation,[26,27] altered calcium homeostasis[16,28] and abnormal glutamatergic input[29-32] are some of the factors that explain the impact of SCA genetic mutations on PC function. Yet, the sequence of pathological events and critical point of PC dysfunction that ultimately leads to the motor deficits seen in SCAs are unclear.

Mouse models of SCAs are a valuable resource to investigate the origins of PC dysfunction by recapitulating clinical features of the disease as well as molecular and cellular phenotypes in a short period of time.[30,33] Here, we sought to investigate the underlying PC pathological events before the onset of ataxia by taking advantage of ATXN1[82Q] mice, a PC-specific mouse model of spinocerebellar ataxia 1 (SCA1).[34] ATXN1[82Q] mice express the human ataxin 1 (*ATXN1*) gene containing 82 CAG repeats under the Purkinje cell protein 2 (Pcp2) promoter. In this mouse model, motor deficits begin at 5 weeks of development with progressive degeneration of PCs.[34-40] Our results revealed that during the pre-ataxia stage impaired PC excitability are followed by abnormal dendritic arborization and weakened mGLUR1 signalling and reduced climbing fibre (CF) connectivity. Moreover, 4-week-old ATXN1[82Q] mice exhibited impaired EBC prior to the ataxia manifestation and this onset coincides with a deficit in PC intrinsic plasticity. Together, these results identify a temporal window of events leading to PC dysfunction that can be used to test novel treatments before irreversible neuronal damage. In addition, our data suggest EBC as a tool to detect early cerebellar dysfunction.

## Materials and methods

### Animals

The transgenic mouse line ATXN1[82Q] (Tg(Pcp2-ATXN1*82Q) 5Horr)[34] used in this study was kindly provided by Dr Harry T. Orr. Experiments were performed on heterozygous transgenic mice of both sexes expressing ATXN1 with an expanded 82 CAG repeats under the *Pcp2* promoter and their wild-type littermates as controls. Mice were kept on an FVB/NHsd background. $F_1$ offspring from crossings between ATXN1[82Q] and C57Bl6/J mice were used for behavioural experiments. Sequencing and PCR reactions to determined CAG repeat length across generations were performed using primers Rep1 (5′-AACTGGAAATGTGGACGTAC-3′) and Rep2 (5′-CAACATGGGCAGTCTGAG-3′) as previously described.[34] For the developmental stages of the study, mice were bred using timed pregnancies and the day of birth was designated postnatal Day 0 (P0). Mice were kept on a 12:12 light/dark cycle, temperature controlled and received water and food *ad libitum*. All animals were handled and kept under conditions that respected the guidelines of the Dutch Ethical Committee (DEC) and Central Committee for Animal Experiments (CCD) for animal experiments and were in accordance with the Institutional Animal Care and Use Committee of Erasmus MC (IACUC) and the European and the Dutch National Legislation. The ARRIVE Reporting guidelines were followed for manuscript preparation.[41]

### Immunohistochemistry

For immunohistochemistry, control and ATXN1[82Q] mice were perfused transcardially and 40-µm slices cut from fixed brains. In addition, to label recorded PCs, free-floating, 250-µm thick sagittal brain slices from *ex vivo* experiments were fixed. Slices were stained for calbindin, ATXN1 and/or VGLUT2. Details of the antibodies, protocols and image acquisition can be found in the Supplementary material.

### Western blotting

Cerebellar tissue from anterior and nodular regions of four control and four ATXN1[82Q] mice at different developmental ages was dissected and immediately frozen in liquid nitrogen. Samples were homogenized with a Dounce homogenizer in ice-cold lysis buffer containing 50 mM Tris-HCl pH 8, 150 mM NaCl, 1% Triton X-100, 0.5% sodium deoxycholate, 0.1% sodium dodecyl sulphate (SDS) and protease inhibitor cocktail (Roche). Protein concentrations were measured using the Pierce BCA protein assay kit (Thermo Fisher). Samples were denatured and proteins were separated by SDS-PAGE (polyacrylamide gel electrophoresis) in Criterion™ TGX Stain-Free™ Gels (Bio-Rad) and transferred onto nitrocellulose membranes with the Trans-Blot® Turbo™ Blotting System (Bio-Rad). Membranes were blocked with 5% bovine serum albumin (BSA; Sigma-Aldrich) in Tris-buffered saline (TBS)–Tween-20 (20 mM Tris-HCl pH 7.5, 150 mM NaCl and 0.1% Tween-20) for 1 h and probed with the following primary antibodies: ATXN1 11750 (gift from Dr Huda Zoghbi, 1:1000, rabbit) or GAPDH (1:1000, mouse, Cell Signaling 97166). Secondary antibodies used were goat Anti-Rabbit Immunoglobulins/horse radish peroxidase (HRP) (1:10000, Agilent Dako P0448) or goat Anti-Mouse Immunoglobulins/HRP (1:10000, Agilent Dako P0447). Proteins were detected by the luminol-based enhanced chemiluminescence method (SuperSignal™ West Femto Maximum Sensitivity Substrate or SuperSignal™ West Dura Extended Duration Substrate, Thermo Fisher). Membranes were stripped with Restore™ PLUS Western Blot Stripping Buffer

(Thermo Fisher). Densitometry of protein bands of interest was normalized to that of GAPDH using the Image Studio Lite software (LI-COR Biosciences). Samples were excluded if the reference protein failed.

## RNA extraction and quantitative PCR

Cerebellar tissue from anterior and nodular regions of 16 control and 12 ATXN1[82Q] mice were collected at P10, P20, P30 and 6 weeks of age from ATXN1[82Q] mice and immediately frozen in liquid nitrogen. Samples were homogenized with TRIzol reagent (Thermo Fisher Scientific) and total RNA was isolated and measured with a NanoDrop 2000 (Thermo Fisher Scientific). From each sample 1 µg of RNA was reverse transcribed into cDNA using the iScript Advanced cDNA Synthesis kit for RT-PCR (Bio-Rad 172-5037). The cDNA was diluted 3-fold and 2 µl were used in a quantitative PCR (qPCR) reaction with the SsoAdvanced Universal Probes Supermix (Bio-Rad 172-5280).

Triplicates were used for each biological sample and *Rn18s*, *Rpl13a* and *PGK* were used as housekeeping genes. Samples were run on a CFX96 Real-time PCR detection system (Bio-Rad). Relative transcript levels were measured using the delta-delta Ct method in order to calculate the relative fold gene expression. Primers and probes used in this experiment were the following: ATXN1[82Q]-forward: 5′-AGAGATAAGCAACGACCTGAAGA-3′; ATXN1[82Q]-reverse: 5′-CCAAAACTTCAACGCTGACC-3′; ATXN1[82Q] probe (Roche 4688597001), Taqman assay IDs Rn18s (Mm03928990_g1), Rpl13a (Mm01612987_g1) and Pkg1 (Mm00435617_m1). Samples were excluded if the reference gene failed.

## *Ex vivo* electrophysiology

Brains of 49 control and 49 ATXN1[82Q] postnatal Day (P) 9–90 mice were used to obtain 250-µm acute sagittal slices for *ex vivo* recordings (Supplementary material). After recovery, slices were transferred to a recording chamber continuously perfused with the oxygenated artificial CSF (ACSF) heated to 34°C (Scientifica). Electrodes were filled with internal solution containing 9 mM KCl, 3.48 mM $MgCl_2$, 4 mM NaCl, 120 mM $K^+$-gluconate, 10 mM HEPES, 28.5 mM sucrose, 4 mM $Na_2ATP$, 0.4 mM $Na_3GTP$ in total pH 7.25–7.35, osmolarity 290–300 mOsmol/kg (Sigma-Aldrich). Biocytin (1 mg/ml) was included to allow the morphological reconstruction of the recorded PCs. For intrinsic plasticity and cell-attached recordings, slices were bathed with ACSF supplemented with synaptic receptor blockers, NMDA receptor antagonist D-AP5 (50 µM), selective and competitive AMPA receptor antagonist NBQX (10 µM), non-competitive GABAA receptor antagonist and glycine receptor inhibitor picrotoxin (100 µM), all from Hello Bio. PCs were held at −65 mV. Intrinsic plasticity[42,43] was induced using a tetanus stimulation of 200 ms, 900 pA pulses at 5 Hz for 8 s. Prior to tetanus, a baseline was recorded by injecting a 500 ms 200–400 pA pulse every 20 s for 5 min. After tetanus, the same current injection was given every 20 s for 30 min. The number of elicited spikes per pulse were counted and averaged for each minute. The results are given as a per cent change from the 5-min baseline. PCs were excluded if the holding potential changed over the experiment by more than 10%. For CF stimulation experiments, after achieving a whole-cell configuration with a PC, a second stimulating electrode was placed in the granular layer near the PC soma; 200-ms sweeps were recorded with a 5-ms electrical stimulation (Dagan BSI-950) occurring at 100 ms. The electrical stimulation started at 1 mA and increased by 500 µA with each sweep. A response was deemed to be a CF response if it both exhibited an all-or-none characteristic and a broad response after the initial spike. After subtracting the mean of the pre-stimulus voltage, the area under the curve of the first spike induced was measured using the *trapz* function in MATLAB.

## Morphological analysis

Molecular layer thickness was determined by measuring in ImageJ the distance from the top of the PC soma to the top of the PC dendritic tree; and the CF height was measured as the distance from the top of the PC soma to the apical edge of the last VGLUT2 puncta. The CF extension was quantified as the percentage of the ratio of the CF height per molecular layer height per image. Analysis of synapse densities (puncta/area) was performed using the 'Analyze Particles' tool in ImageJ software to quantify the number of VGLUT2 puncta in a region of interest and this number was then divided by the area ($\mu m^2$) of the region of interest in the cerebellar cortex.

To quantify the area of a PC, the maximum projection of each image was thresholded in ImageJ to fit the area of the cell and measured. To quantify dendritic arborization the maximum projection of z-stack images of single cells were analysed with the Sholl analysis macro implemented in ImageJ software.

## Behavioural tests

### Balance beam test

For the balance beam test, ATXN1[82Q] and respective controls were tested at 3, 4, 6, 12 and 18 weeks of age. The test consisted of two training days and one testing day. Mice were tested on a 1-m long 6- or 12-mm diameter balance beam situated between two elevated platforms 50 cm above the surface. A cage was placed at the end of the beam as a finish point. The parameters analysed were the time to cross and the number of foot slips per run.

### Compensatory eye movement recordings

Control and ATXN1[82Q] mice (3 or 4 weeks of age on the first day of experiment) were used to perform and analyse compensatory eye movement recordings by a researcher blind to group categorization, which were described in detail previously.[44,45] Details of pedestal placement and behavioural apparatus can be found in the Supplementary material. Mice were tested for baseline optokinetic, vestibulocular and visual vestibulocular responses. Motor performance in response to these stimulations was evaluated by calculating the gain (eye velocity/stimulus velocity) and phase (eye to stimulus in degrees) of the response. To study motor learning, mice were subjected to a mismatch between visual and vestibular input to adapt the vestibulocular response. Gain and phase values of eye movements were calculated using custom MATLAB scripts (MathWorks, https://github.com/MSchonewille/iMove).[44]

### Eyeblink conditioning

Control and ATXN1[82Q] mice (3, 4, 6 or 12 weeks of age on the first day of experiment) were used to perform and analyse EBC behavioural tests by a researcher blind to group categorization as previously described.[46] Details of pedestal placement and behavioural apparatus can be found in the Supplementary material. The conditioned stimulus (CS) was a blue LED light (CS duration: 280 ms) placed 10 cm in front of the mouse's head. The unconditioned stimulus (US) was a weak air-puff (30 psi, 30-ms duration), which

was positioned at 5 mm from the centre of the left cornea. The interval between the onset of CS and that of the US was set at 250 ms. Preventive eyelid closure before US time was considered a conditioned response (CR). Individual eyeblink traces were analysed with a custom written script in MATLAB R2018a.

### Statistical analysis

Data are presented as the mean ± SEM. Normality of the distributions was verified via the Shapiro–Wilk test and equal variances were tested with the *F*-test. For normally distributed data, statistical significance was determined by the two-way ANOVA with multiple comparisons or mixed-effects test with repeated measures. If the data were not normally distributed, statistical significance was calculated using the Kruskal–Wallis test with multiple comparisons. The minimum level of significance accepted for all tests was $P < 0.05$. Statistical analyses were performed using GraphPad Prism software (version 8.0.0). For each experiment, the sample size and statistical tests used are summarized in Supplementary Table 1. Total group size for behavioural tests was determined by power analysis to be 12–26 and for electrophysiological experiments to be 12–30.

### Data availability

The authors confirm that the data supporting the findings of this study are available within the article and its Supplementary material. The data that support the findings of this study are also available from the corresponding author upon reasonable request.

## Results

### Differential expression of ATXN1[82Q] transgene in ATXN1[82Q] mice

The *Pcp2* promoter used in the *ATXN1[82Q]* mouse model drives mutant ATXN1 expression in the vast majority of PCs, but we have previously identified relatively minimal transgene expression in the flocculonodular region in the adult.[47] To better understand the levels and location of *ATXN1[82Q]* transgene expression during the pre-ataxia period, we investigated the levels of mRNA and protein in a spatiotemporal manner. Transgenic *ATXN1[82Q]* mRNA expression levels could already be detected as early as P10 (Supplementary Fig. 1A). These levels were similar between anterior (lobules I–III) and nodular (lobules IX–X) cerebellar regions of ATXN1[82Q] mice at P10 and P20. At P30 and 6 weeks of age, the mRNA levels of the transgene were significantly higher in the anterior regions compared with the nodular regions (Supplementary Fig. 1A). Quantification of ATXN1 protein levels revealed significantly higher ATXN1[82Q] protein values in the anterior regions of ATXN1[82Q] mice cerebella earlier, at P20 (Supplementary Fig. 1B and C). In accordance with our protein expression data, immunostaining for ATXN1[82Q] was detected in PCs in both the anterior vermis (I–III) and posterior/nodular vermis (VIII–X) during the different postnatal ages (Fig. 1A and C and Supplementary Fig. 2A and B). However, in line with adult expression,[47] posterior/nodular lobules have a more irregular pattern of ATXN1[82Q] expression with several non-labelled regions in the vermis, when compared with the anterior regions. At P10, the strongest mutant protein expression is located in the vermal region, but from P20 to 6 weeks of age ATXN1[82Q] expression is stronger in the simplex lobule and crus I (Supplementary Fig. 2C). In the flocculus, the levels of ATXN1[82Q] are absent at P10, but from P20 it is possible to identify a few positive PCs (Supplementary Fig. 2D). The ATXN1[82Q] protein was initially detected mainly in the PC nuclei and from P20 the staining was also present in the dendrites (Fig. 1B and D). This staining co-localized with PC-specific marker calbindin. Additionally, we validated that mutant animals from different generations show no change in CAG repeat length, demonstrating that this region is stably transmitted across generations as described previously (Supplementary Fig. 1D and E).[34] After confirming that the differences in transgene expression in our model are already present in the pre-ataxia period, we continued our study by separately analysing regions with more homogenous, high transgene levels (anterior lobules I–III) and regions with low ATXN1[82Q] levels (nodular lobules IX–X).

### PC dendrite arborization is stunted from the third postnatal week in ATXN1[82Q] mice

During the first postnatal weeks the development of PC activity correlates with the growth of its massive dendritic arbour, which is affected in adult ATXN1[82Q] mice.[34] Thus, we aimed to determine when the first signs of abnormal PC morphology appeared in regions with high ATXN1[82Q] transgene versus regions with lower transgene expression. We analysed dendritic morphology of PCs from lobules I–III in control and ATXN1[82Q] mice at different pre-ataxia ages. Biocytin-filled PCs were analysed to measure dendritic arbour complexity, maximum dendrite length from the cell soma and PC area (soma and dendrite), using Sholl analysis.[48] No differences were observed in dendritic complexity (Fig. 2A and B), maximum length (Fig. 2C) and area (Fig. 2D) between control and ATXN1[82Q] PCs at P10–P14 in the anterior regions of the cerebellum. In contrast, dendritic complexity was significantly reduced in P15–P21 ATXN1[82Q] PCs compared with control PCs (Fig. 2A and E) as well as maximum length and PC area (Fig. 2F and G). Similar results were observed in the older age group (Fig. 2A, and H–J). In the nodular regions of the cerebellum, there were no significant differences in the number of intersections between control and mutant in the pre-ataxia stage (Supplementary Fig. 3). In the older ages, we detected a small but significant decrease in PC area in the ATXN1[82Q] mice when compared with the controls (Supplementary Fig. 3J).

### PC intrinsic excitability and spontaneous firing are both reduced in the second postnatal week in ATXN1[82Q] mice

Impaired physiological activity of PCs has been reported in different models of SCA and precedes behavioural pathology.[37,49] To determine when during the pre-ataxia stage differences in intrinsic excitability arise, we performed whole-cell recordings in PCs in lobules I–III and X from P10 to P60. To test for intrinsic excitability, we injected steps of increasing current.[50] In all control groups, we found a difference in intrinsic excitability between anterior and posterior/nodular vermis, as reported previously.[45] ATXN1[82Q] PCs demonstrate a significantly lower elicited action potential count when compared with control PCs in the anterior cerebellum (Fig. 3A and B). These differences were detected as early as P10 and continued into adulthood (Fig. 3C). No differences in PC intrinsic excitability were detected in the nodular region between ATXN1[82Q] PCs and control during the time points analysed (Supplementary Fig. 4), in line with previous findings comparing nodular PCs between ATXN1[82Q] PCs and controls.[26] The impaired intrinsic excitability in anterior ATXN1[82Q] PCs could be the result of changes in the action potential threshold and/or the membrane resistance. Hence, we further characterized the differences in current integration by testing both in our dataset. No significant differences were found between the membrane resistance of ATXN1[82Q] and control PCs at any age (Fig. 3E). The action potential threshold

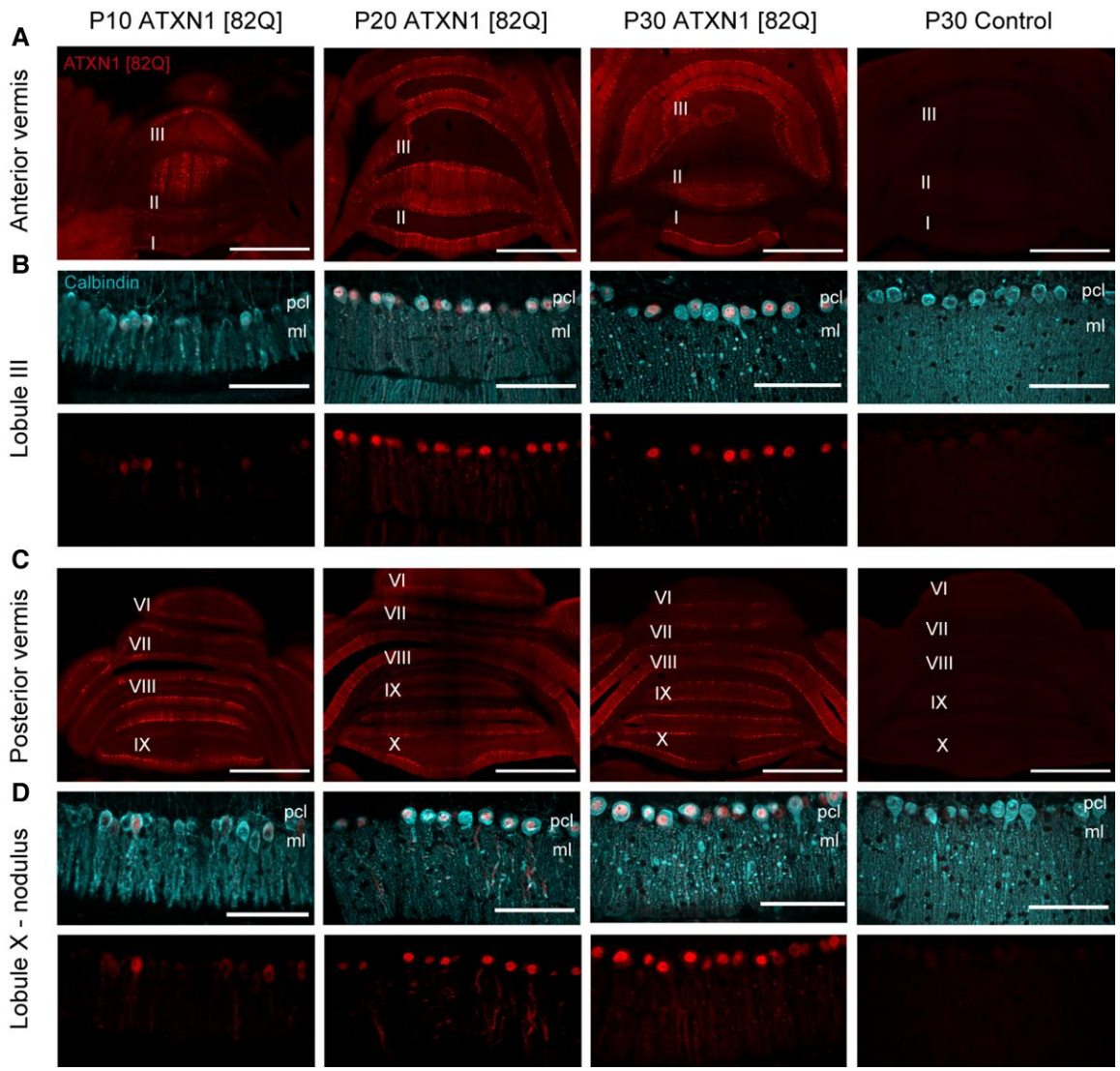


**Figure 1 Differential expression of ATXN1[82Q] protein in the cerebellum of ATXN1[82Q] mice during the asymptomatic period.** Representative photomicrographs of ATXN1[82Q] expression in PCs of the anterior (**A**) and posterior vermis (**C**) in ATXN1[82Q] and control mice at different developmental ages (scale bar = 1000 µm). Detailed images of PCs in lobule III (**B**) and lobule X (**D**) expressing ATXN1[82Q] and calbindin at different developmental ages (scale bar = 100 µm). Age groups: P10, P20 and P30. Cerebellar lobules are labelled with roman numerals. ml = molecular layer; pcl = Purkinje cell layer.

was found to be higher in adult lobule I–III ATXN1[82Q] PCs, but not significantly different in juvenile mice (Fig. 3D). Resistance in itself, however, would support higher intrinsic excitability, and thus neither membrane resistance nor the action potential threshold can explain the impaired intrinsic excitability in anterior ATXN1[82Q] PCs. To verify if deficits in PC firing are also present in conditions where the internal milieu of the cell is not affected by the whole-cell configuration, we additionally recorded spontaneous firing of lobule III PCs using a cell-attached configuration with synaptic transmission blocked. Indeed, spontaneous firing rate was significantly lower in ATXN1[82Q] PCs at both P21 and over P30, while CV2 was not significantly different at any age (Supplementary Fig. 5).

## Abnormal eyeblink conditioning in ATXN1[82Q] mice precedes the ataxic phenotype

To determine the onset of ataxia in our cohort of SCA1 mice, we measured motor performance of ATXN1[82Q] with the balance beam test. Consistent with previous reports, mice expressing *ATXN1[82Q]* showed significant impartment in the balance beam from 6 weeks of age onwards when compared with the controls (Supplementary Fig. 6).[34-40]

Our results revealed that in the ATXN1[82Q] model, PC pathology in the pre-ataxia stage[34-40] is more pronounced in regions with higher levels of the transgene. Because abnormal physiology and morphology were detected within the first three postnatal weeks, we asked if motor tests more sensitive to cerebellar changes could detect functional impairments prior to ataxia onset. To assess the integrity of cerebellum-dependent behaviours, we subjected ATXN1[82Q] and control littermate mice to EBC and vestibulocular response adaptation, both established cerebellum-dependent learning tasks.

In the EBC task, a visual CS, a 280-ms LED light, is paired with an eyeblink eliciting US, a 30-ms air puff delivered to the mouse cornea co-terminating with the CS (Fig. 4A and B). Naïve mice are

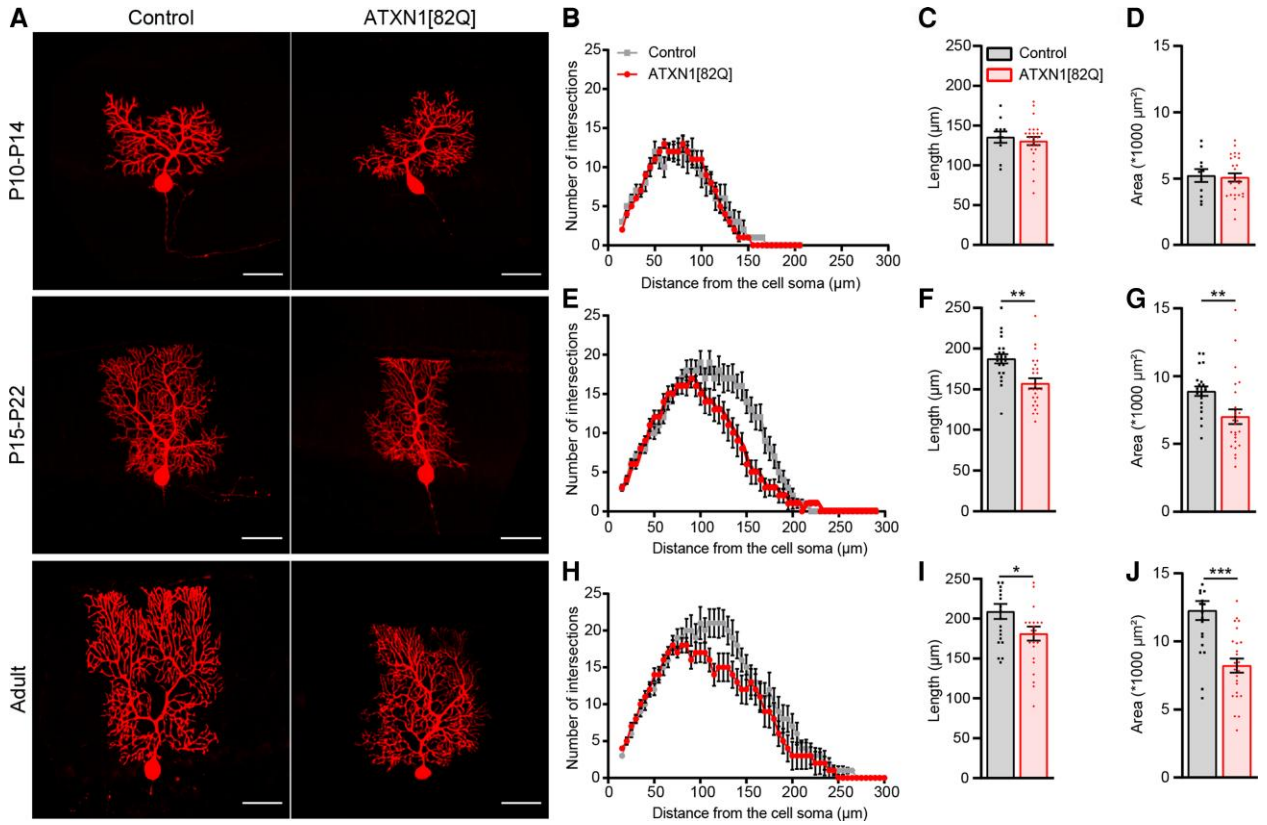


**Figure 2 PC complexity is reduced in the anterior cerebellum of ATXN1[82Q] mice from the third postnatal week.** (**A**) Representative photomicrographs of PCs filled with biocytin in lobules I, II and III in three age groups in control and ATXN1[82Q] mice (scale bar = 50 µm). (**B**, **E** and **H**) Sholl analysis, (**C**, **F** and **I**) longest dendrite length and (**D**, **G** and **J**) area quantification of PCs in three age groups for control and ATXN1[82Q] mice. Age groups: P10–P14, P15–22 and adult (between 5 and 9 weeks old). Data from individual cells are expressed as mean ± SEM, for values see Supplementary Table 1. $^{*}P < 0.05$, $^{**}P < 0.001$, $^{***}P < 0.0001$, unpaired two-tailed *t*-test or two-tailed Mann–Whitney test.

unresponsive to the CS, but they produce an unconditioned eyelid reflex (unconditioned response, UR) in response to the air puff only (US). After several sessions of training, mice can prompt a preventative eyelid closure, or conditioned response (CR), when presented only with the CS (Fig. 4B).[51-53] We compared the acquisition of CRs in control and ATXN1[82Q] mice at 3, 4, 6 and 12 weeks of age. As expected, 6- and 12 week-old ATXN1[82Q] mice presented a significantly lower CR percentage when compared with their corresponding control animals (Fig. 4C). Likewise, the fraction of eyelid closure was significantly reduced in ATXN1[82Q] mice (Fig. 4D). The reduced EBC learning in the 6- and 12-week-old ATXN1[82Q] mice is in line with the progressive level of PC degeneration observed at these ages as well as the increased severe ataxic phenotype as previously described.[35,47] Interestingly, 4-week-old ATXN1[82Q] animals also already had a diminished rate of EBC acquisition, both in CR percentage and fraction of eyelid closure (Fig. 4C and D). However, at 3 weeks of age, despite the physiological and morphological changes observed in PCs in the second and third postnatal weeks, respectively, there were no differences in the learning abilities between genotypes (Fig. 4C and D and Supplementary Fig. 7A). The analysis of the unconditional response timing and onset between both groups at 3, 4 and 6 weeks showed no difference, ruling out the possibility that mutant mice had a reduced ability to close the eyelid (Supplementary Fig. 7B). Our data suggest that the anterior eyeblink region is already vulnerable to ATXN1[82Q]-driven pathogenesis prior to the ataxia stage.

In addition, we tested the ATXN1[82Q] model with a second cerebellum-dependent learning test: the vestibulo-ocular reflex adaptation. Eye movement-related areas are located in the vestibulocerebellum that comprises the flocculonodular lobe.[54] The PCs in this structure receive vestibular and visual input and use information about head movement to influence eye movement.[55] Recently, we have shown that PC degeneration in these regions is relatively mild and that compensatory eye movements and their adaptation were preserved in adult ATXN1[82Q] mice.[47] We tested if young control littermate and ATXN1[82Q] animals, 3 and 4 weeks old, would differ in their compensatory eye movements. As expected, there were no differences between genotypes in both gain and phase in the optokinetic reflex, vestibular–ocular reflex, and visual vestibular–ocular reflex (Supplementary Fig. 8A, C, E, G and I). To further challenge these mice, we subjected them to a gain-increase vestibular–ocular reflex adaptation protocol. The test measures if mice can learn to increase their vestibular–ocular reflex over time using visual feedback (visual and vestibular stimulation out-of-phase).[44,56-58] As expected, both control and mutant mice at 3 and 4 weeks old were able to adapt their vestibular–ocular reflex (Supplementary Fig. 8B, D, F, H and J). Overall, juvenile ATXN1[82Q] mice showed no defects in compensatory eye movements and adaptation. This is in accordance with the preservation of physiological and morphological features of PC in the

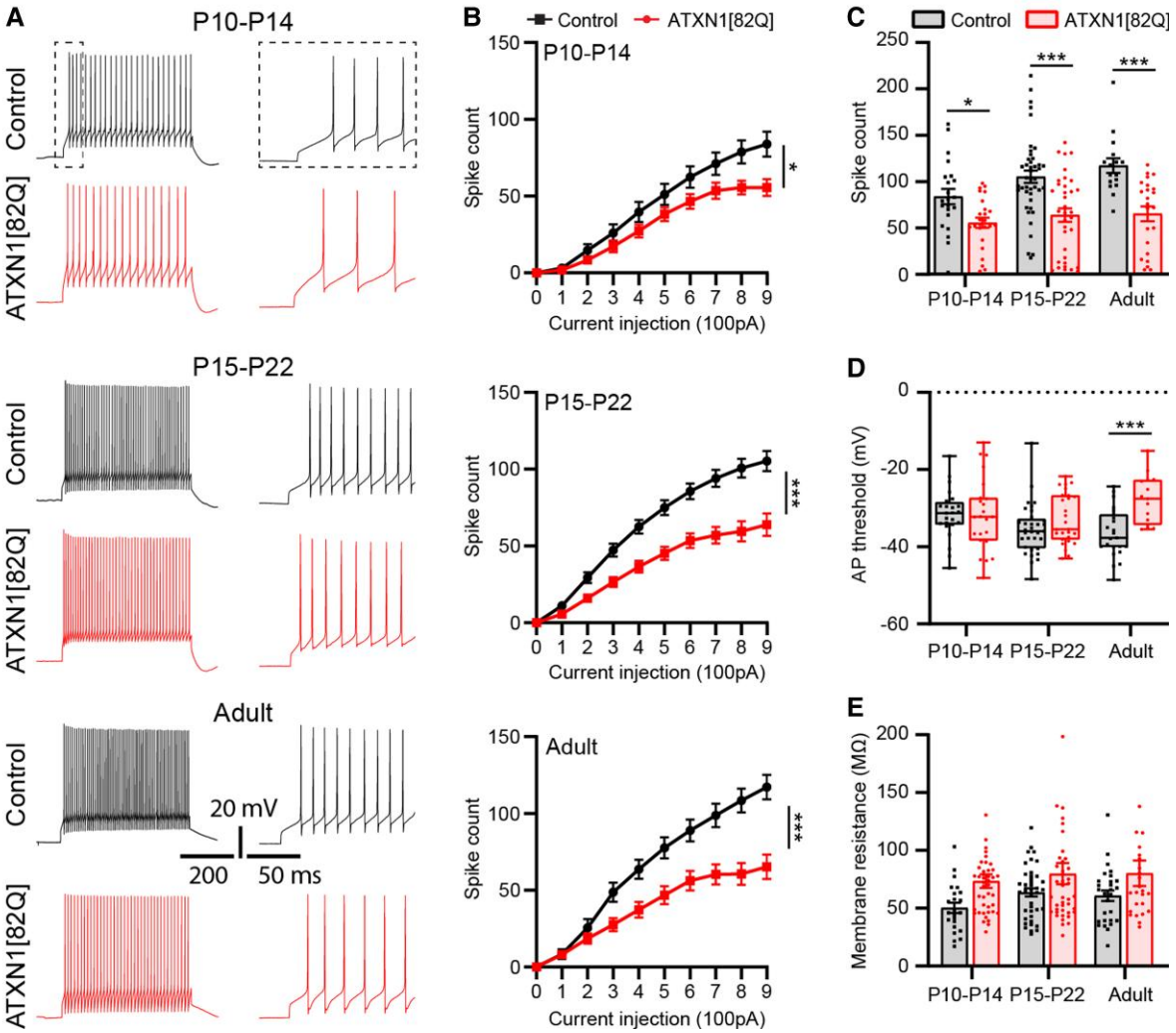


**Figure 3 Intrinsic excitability is reduced in PCs located in the anterior cerebellum of ATXN1[82Q] mice from the second postnatal week.** (**A**) Example traces of current injection recordings of PCs in anterior lobules I, II and III of control and ATXN1[82Q] mice in three age groups. (**B**) Spike count of PCs from control and ATXN1[82Q] mice in response to a series of current injections with 100 pA increments in three age groups. (**C**) Mean spike count of the last current injection step, (**D**) Action potential (AP) threshold and (**E**) membrane resistance of control and ATXN1[82Q] mice in three age groups. Age groups: P10–P14, P15–22 and adult (between 5 and 9 weeks old). Data from individual cells are expressed as mean ± SEM, for values see Supplementary Table 1. *P < 0.05 and ***P < 0.0001, two-way ANOVA and mixed-model test.

flocculonodular lobes, which is most likely due to the partial transgene expression observed (Supplementary Fig. 2D).

## The onset of climbing fibre degeneration follows PC dysfunction in ATXN1[82Q] mice

An additional pathological feature in the cerebellum of SCA1 patients is the degeneration of CFs and therefore subsequent deficiency in CF–PC connectivity.[59,60] This feature has been observed in the ATXN1[82Q] mouse model at 12 weeks of age.[61-64] PCs in lobules IV–V of the anterior vermis and the simplex lobule in the hemispheres integrate the inputs from climbing and mossy fibres and drive the EBC responses.[65,66] Therefore, one could hypothesize that the CF degeneration in the ATXN1[82Q] model during the pre-ataxia stage contributes to the abnormal EBC performance at 4 weeks of age. To test this, we followed the progression of CF degeneration by performing immunostainings in the cerebellar cortex of control and ATXN1[82Q] mice from anterior lobules I–III at different developmental ages. Using VGLUT2 as a marker for CF terminals, we found no differences in the percentage of area covered by VGLUT2-positive puncta from P5 to P10, a time when the CF transfers from the soma to the dendrite. At P20 and P30, when multiple CF innervation is converted into single innervation, there was a significant reduction in the percentage of VGLUT2-positive puncta in the mutant ATXN1[82Q] cerebellum when compared with control (Fig. 5A and B). This was not caused by an equivalent thinning of the molecular layer, which only showed a decrease in thickness at P30 (Fig. 5A and C). In line with the loss of VGLUT2-positive puncta, the percentage of CF extension into the molecular layer was significantly reduced at P30 in the mutant mice (Fig. 5A and D). Interestingly, we also observed a reduction of VGLUT2-positive puncta, CF extension and molecular layer thickness at P30 in the nodular lobules of ATXN1[82Q] mice (Supplementary Fig. 9).

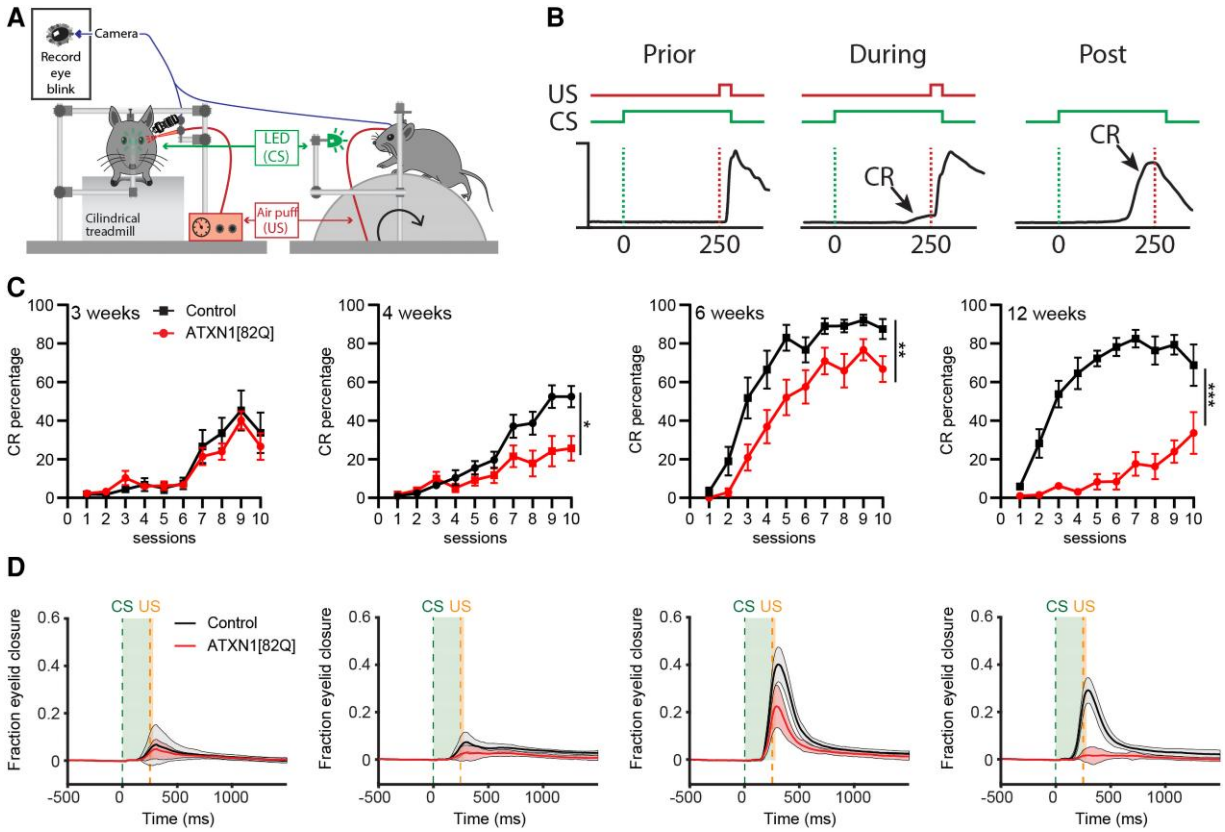


**Figure 4 EBC is impaired in pre-ataxic ATXN1[82Q] mice.** (**A**) Schematic illustration of the EBC recording setup. (**B**) By repeated pairings of the CS and the US, mice will learn to close their eye in response to the CS alone, eliciting the CR. (**C**) CR% for control and ATXN1[82Q] mice during 10 training sessions over 5 days of training. (**D**) Comparison of fraction of eyelid closure between control and ATXN1[82Q] mice. Age groups and number of mice (*n*, control versus ATXN1[82Q]): 3 weeks ($n = 12$ versus 11), 4 weeks ($n = 16$ versus 12), 6 weeks ($n = 10$ versus 11) and 12 weeks old ($n = 8$ versus 10) mice. Data are expressed as mean ± SEM, for values see Supplementary Table 1. $^{*}P < 0.05$, $^{**}P < 0.001$, $^{***}P < 0.0001$, mixed-model test.

In order to determine whether there is any functional impact of the observed CF degeneration, we stimulated CFs during whole-cell recordings of PCs in lobule III at P21 and over P30. The response of a PC to CF activity can be recorded in *ex vivo* slices by stimulating the CF axon within the granular layer near the recorded PC.[67-69] Area under the curve analysis showed no significant difference at P21 between control and ATXN1[82Q] PCs, but CF response was significantly smaller over P30 (Supplementary Fig. 10). Together, these results demonstrate that CF degeneration strongly correlates with EBC impairment prior to ataxia, but could be independent from PC dysfunction.

Because of the PC specificity of this ATXN1[82Q] mouse model, CF degeneration most likely results from a defective metabotropic glutamate receptor subtype 1 (mGluR1) to protein kinase C gamma ($PKC\gamma$) cascade in PCs (Supplementary Fig. 11E). This pathway is necessary for the elimination of redundant CF synapses from proximal regions of PC dendrites from P15 to P30.[70-73] Faulty glutamatergic signalling has been demonstrated in several models of SCA disease.[10,29,39,71,73-77] Hence, we explore the possibility that some proteins underlying glutamatergic signalling in PCs have an altered expression in the pre-ataxia period as well. Indeed, our data demonstrated that IP3R1 levels were reduced in the ATXN1[82Q] cerebella from P20 while mGLUR1, HOMER3 and TRPC3 expression were reduced at P30 in the anterior regions of the cerebellum (Supplementary Figs 11 and 12).

## Reduced PC intrinsic plasticity precedes the ataxic phenotype

Finally, to examine a physiological basis of learning and learning deficits at the neural level, we tested PCs for intrinsic plasticity[42,43] before and after the onset of abnormal behaviour in EBC. Intrinsic plasticity is a form of neural learning that can be elicited through direct excitation of the neuron.[78] PCs readily undergo intrinsic plasticity[79,80] and selective mutations that attenuate intrinsic plasticity impair EBC, but not VOR adaptation in adult mice.[43] Moreover, intrinsic plasticity is precluded in PCs after EBC, suggesting that the conditioning has already induced this form of plasticity and precludes any additional physiological change.[42] Therefore, we aimed to investigate this form of learning in ATXN1[82Q] PCs. We found that intrinsic plasticity could not be induced in ATXN1[82Q] lobule I–III PCs compared to controls at P30–P45 (Fig. 6B and D). However, at P20, moderate intrinsic plasticity could be induced in both ATXN1[82Q] PCs and control PCs (Fig. 6A and C) and intrinsic plasticity could be readily induced in ATXN1[82Q] lobule X PCs (Supplementary Fig. 13). The moderate levels of intrinsic plasticity and learning abilities in EBC at P20 compared with adolescent and adult stages, together with the onset of deficits at P30 in lobule I–III but not lobule X PCs, support a link between deficits in intrinsic plasticity and EBC.

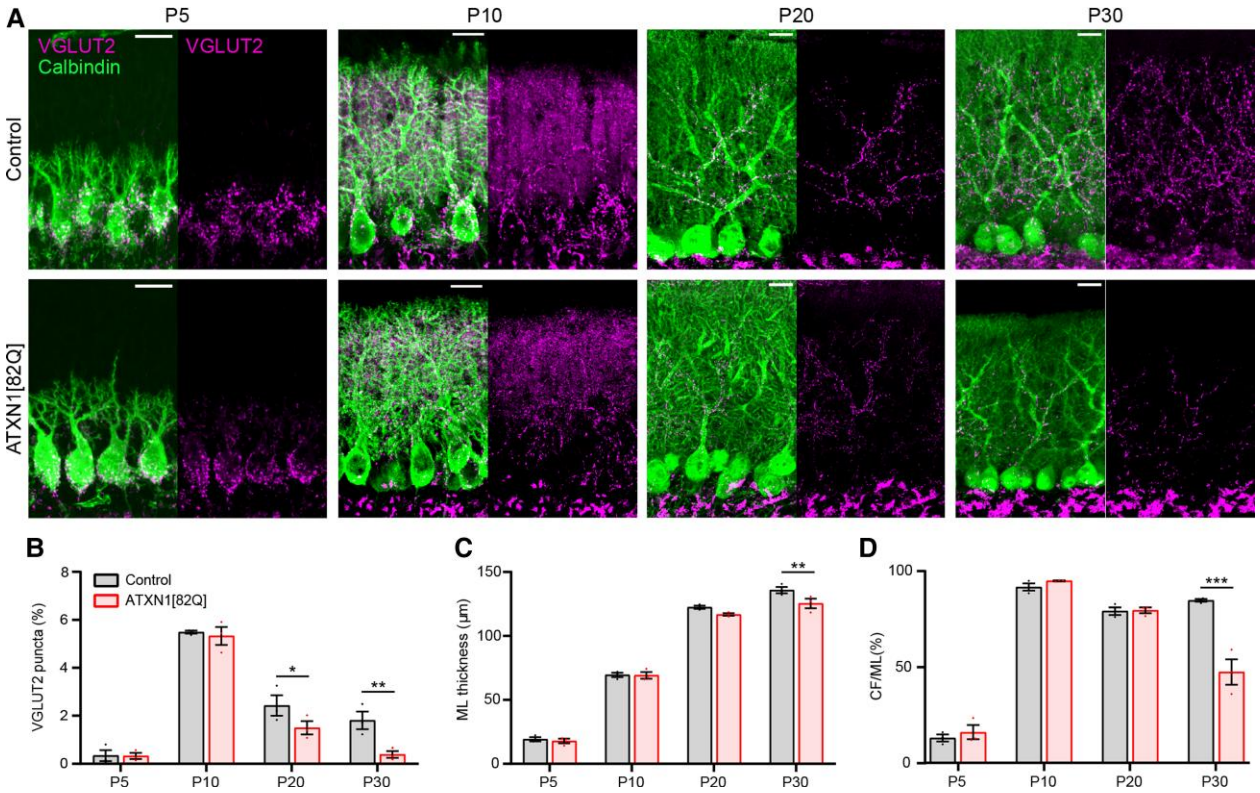


**Figure 5 CF degeneration starts at 3 weeks of age in the anterior cerebellum of ATXN1[82Q] mice.** (**A**) Representative photomicrographs of CFs (VGLUT2 staining) and PCs (calbindin) in lobules I and II or III at different age groups in control and ATXN1[82Q] mice (scale bar = 20 µm). (**B**) VGLUT2 puncta per area of the region of interest, (**C**) molecular layer (ML) thickness and (**D**) CF extension per ML thickness quantification. Age groups: P5, P10, P20 and P30. Data per image are expressed as mean ± SEM, for values see Supplementary Table 1. *P < 0.05, **P < 0.001, ***P < 0.0001, two-way ANOVA.

## Discussion

In this study we investigated the sequence of pathological events leading to PC dysfunction and ataxia in a mouse model of SCA1. Spatiotemporal characterization of the ATXN1[82Q] SCA1 mouse model revealed high levels of the mutant ATXN1[82Q] during the pre-ataxia stage, particularly in areas such as the anterior vermis, lobule simplex and crus I. In this mouse model, the expression of the toxic protein causes a reduction of PC intrinsic excitability in the second week, which precedes the atrophy of dendrite arbours and aberrant metabotropic glutamate signalling starting in the third week and the degeneration of CFs in the fourth week. Functional analyses revealed that the mutant ATXN1[82Q] protein from the fourth week disrupts the intrinsic plasticity of PCs that, with abnormal CF innervation, culminates in impaired EBC motor learning before the onset of ataxia. These data suggest that an accumulation of PC dysfunction climaxes with the loss of intrinsic excitability to produce the presentation of the ataxic phenotype.

The dysfunction of PCs in the ATXN1[82Q] mouse model starts with dysregulation of transcription as described before.[28,29,40,81] Transcripts of *Itpr1* and *Trpc3*, involved in the maintenance of calcium homeostasis, were found to be downregulated at 2 and 4 weeks of age, respectively.[28] Our results show that these proteins are both downregulated most prominently in the anterior vermis at 4 weeks of age, and the reduction of IP3R1 in the anterior vermis starts at 3 weeks of age (Supplementary Figs 11 and 12). In PCs, activation of metabotropic glutamate receptors (mGLURs) increase calcium signalling by initiating the protein kinase C (PKC) pathway, which in turn triggers calcium channels such as the transient receptor potential type 3 (TRPC3) and, ultimately, inositol 14,5-trisphosphate receptors (IP3R1)are activated.[82] Abnormal calcium levels have been linked with changes in PC intrinsic activity[83,84] and to various forms of ataxia in different SCAs.[27] PC-specific deletion of TRPC3 reduced the intrinsic excitability of PCs in the anterior, but not the nodular lobules,[85] indicating that TRPC3 could be a factor in the deficit, but presumably only later in development when the levels of TRPC3 are reduced. However, our data revealed a reduction of intrinsic firing frequency in PCs expressing toxic ATXN1[82Q] protein already from P10 to P14 and spontaneous firing frequency before 3 weeks of age. We did not find any significant difference in membrane resistance at any age, but membrane resistance has been shown to be higher in PCs of older ATXN1[82Q] mice as the cellular atrophy progresses.[86] Chopra *et al.*[26] related changes in PC intrinsic activity in this mouse model with a selective dysregulation of ion channels in particular $Ca_v3.1$, IP3R1 and BK channels. Overall, changes in the expression of channels and receptors that regulate membrane excitability precede morphological and motor impairments and should be considered primary targets for therapeutic endeavours. The subsequent pathological feature we detected was a change in PC dendritic morphology, starting from P15 in PCs expressing higher levels of toxic protein. Changes in dendritic morphology have been associated with reduced expression of potassium channels and increased dendritic excitability in this SCA1 model.[87] Subsequently, at 4 weeks of age, CF synapses were reduced in both anterior and nodular cerebellar regions of the ATXN1[82Q] model. Given that

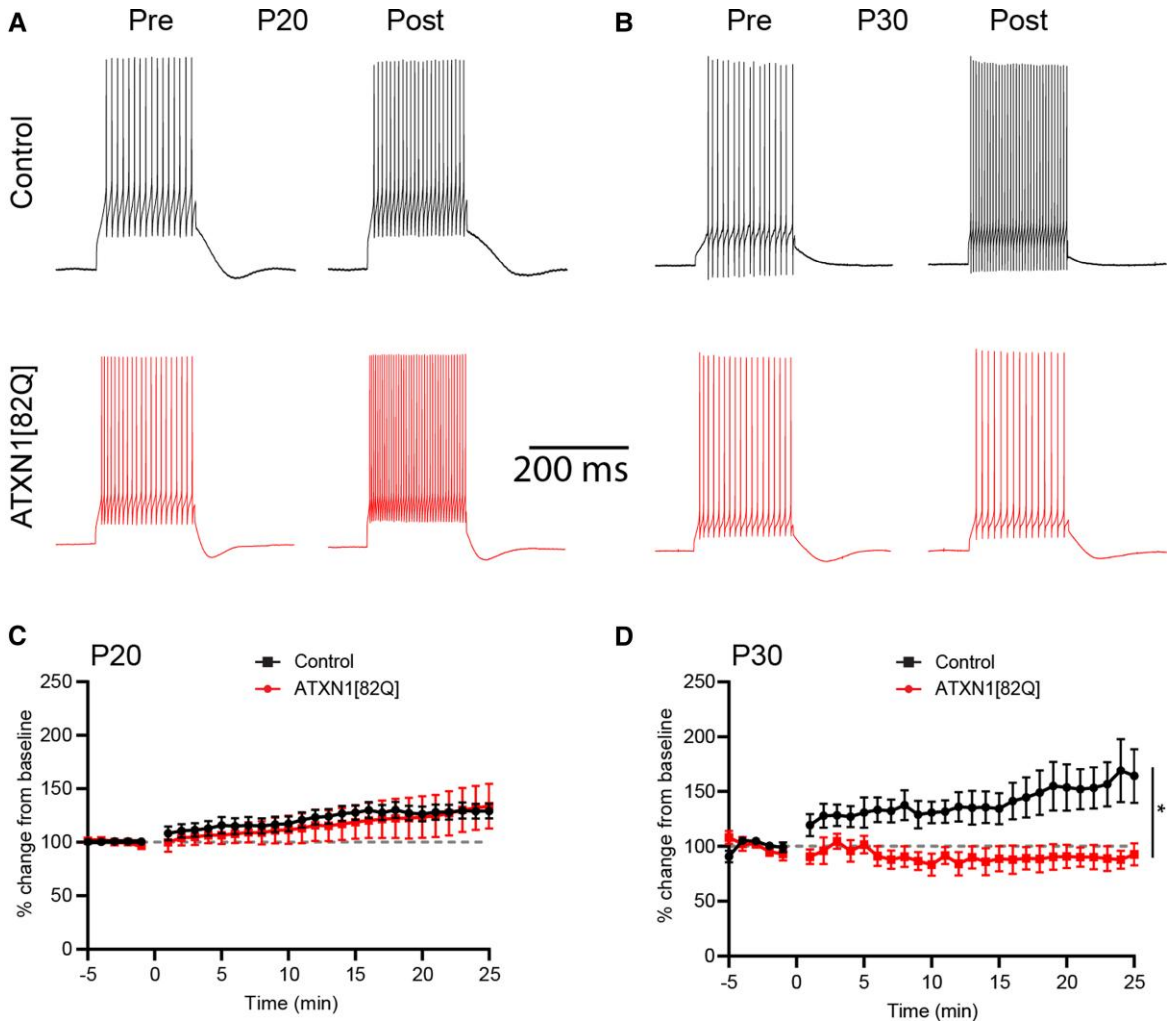


**Figure 6 Intrinsic plasticity is disrupted in ATXN1[82Q] PCs at P30.** (**A** and **B**) Representative traces of induced action potentials before and after tetanus stimulation in control and ATXN1[82Q] PCs at P20 (**A**) and P30–P45 (**B**). Action potentials were evoked by 500 ms and 200–400 pA current pulses (adjusted to drive ~10–15 spikes) every 20 s. Intrinsic plasticity was induced using a tetanus stimulation of 200 ms, 900-pA pulses at 5 Hz for 8 s. (**C**) P20 and (**D**) P30 percentage change of induced action potential number relative to baseline (5 min) and followed over time for at least 25 min. Data from individual cells are expressed as mean ± SEM, number of cells (*n*) for controls versus ATXN1[82Q] is $n = 10$ versus 8 for P20, $n = 6$ versus 7 for P30; *$P < 0.05$, two-way ANOVA (for values see Supplementary Table 1).

the toxic protein is only expressed in PCs in the ATXN1[82Q] mouse model, not in the olivary neurons that give rise to the CFs, this is a direct result of PC dysfunction. Changes in CF input in SCA have been reported before[32,61,63] and the data presented here suggest altered mGLUR1 signalling pathway as a mechanism. Postsynaptic mGLURs are vital for the elimination of redundant CF synapses that occurs between the third and fourth weeks in the mouse.[30,71,73,88] Presynaptic consequences of a mutation that exclusively affects the postsynaptic PC have been found before in the ATXN1[82Q] mouse model, in the form of inappropriate parallel fibre distribution[63] and changes in insulin-like growth factor.[89] Hence, in can be concluded that a combination of both deficient intrinsic activity and abnormal input underlies cerebellar dysfunction in many SCAs.[50]

In this study, we dissect the pathogenesis and show that faulty PC intrinsic plasticity correlates, in a temporally specific manner, with impaired EBC before the onset of ataxia in the ATXN1[82Q] mice. EBC is a form of associative learning uniquely dependent on the cerebellum for information processing[90,91] and deficits in eyeblink responses are known to be present in patients with cerebellar deficits.[92-95] Classically, alterations in synaptic strength are considered to form the basis for cerebellar motor learning.[96,97] More recently, a combination of synaptic plasticity and plasticity of intrinsic membrane excitability, or intrinsic plasticity, is thought to be the mechanism underlying cerebellar learning.[98,99] The involvement of intrinsic mechanisms has been shown by the increase of membrane excitability after EBC in rabbits[79,100] and mice[42] and the fact that EBC is impaired following mutations that ablate intrinsic plasticity.[42,43] Our experiments provide three arguments supporting the idea that in ATXN1[82Q] mice intrinsic plasticity is responsible for the pre-ataxia deficit in EBC: (i) several features of PC development are affected before or at P20, but a behavioural phenotype has never been reported for this period; (ii) at P20 the levels of intrinsic plasticity and EBC are relatively low compared to adolescent and adult mice, and not significantly different between ATXN1[82Q] and control mice; and (iii) the level of intrinsic plasticity and EBC in control mice, but not that in ATXN1[82Q] mice, increases from P20 to P30, causing a significant difference in both comparisons. If PC intrinsic plasticity is indeed an important factor in the onset of ataxia, novel therapeutic targets

can be tested. For instance, SK2 channels are known to mediate PC intrinsic plasticity by controlling the after-hyperpolarization following an action potential.[80,101,102] Mice with a PC-specific deletion of SK2 channels showed impaired EBC and ablation of PCs intrinsic plasticity.[43] SK2 channel activity is suggested to be suboptimal in episodic ataxia type 2 and SK channel activators 1-ethyl-2-benzimidazolinone and chlorzoxazone were able to improve motor coordination in tottering and ducky mice.[83,103] Calcium regulation in general may contribute to the dysfunctional intrinsic plasticity in ATXN1[82Q] PCs. We find that expression of important proteins for calcium regulation, such as IP3R1, are altered around the same time as we observe the intrinsic plasticity deficit. It has been shown that calcium regulation and proteins involved in calcium regulation are altered in SCA1 and other ataxias.[16,28,104] Additionally, our finding of a clear deficit in EBC before the onset of ataxia supports the use of EBC as a clinical tool to detect subtle cerebellar changes in humans before severe motor impairments manifest. A recent clinical study found that EBC is impaired in preclinical carriers of a SCA3 mutation,[9] supporting the use of EBC as an early marker, potentially for a broader range of (spinocerebellar) ataxias. Treatment of such genetic disorders, e.g. through the use of gene therapy, will require an early marker that allows for identification of future problems. Moreover, knowledge of the most optimal time window prior to severe disease onset, as well as quantifiable parameters to track disease progression, will be essential for any potential treatment option. Antisense oligonucleotide (ASO) therapy was able to delay the onset of phenotypes in mouse models of SCA2 when provided at a time prior to their typical appearance. ASO therapy is currently successfully applied for diseases with a well-defined onset and disease progression, such as Duchenne muscular dystrophy and spinal muscular atrophy.[11,105,106] The data presented here demonstrate that many pathological features can be present prior to the apparent disease phenotype. Treatment of the specific pathology prior to its appearance should be a goal for treatment of diseases like SCAs.

## Acknowledgements

We thank Dr Geeske van der Woerden and Dr Dick Jaarsma for comments on the manuscript and Fedde van Oord, Pascal Gunsch, Pasquale Paletta and Eleanor van der Horst for technical assistance.

## Funding

This work is supported by grants from the H2020 European Research Council (ERC-Stg #680235) (M.S.); Nederlandse Organisatie voor Wetenschappelijk Onderzoek, ZonMw Off-road (ZonMW-451001027), OCENW.XS5.121 and Incentive Grant for Women in STEM (19498) (C.O.); Nederlandse Organisatie voor Wetenschappelijk Onderzoek (016.Veni.192.270 and OCENW.XS21.1.087) and Erasmus MC Fellowship (J.J.W.) and NRF-Nuffic Doctoral Scholarship (grant number 111611) (H.L.).

## Competing interests

The authors report no competing interests.

## Supplementary material

Supplementary material is available at *Brain* online.

## References

1. Harding AE. Classification of the hereditary ataxias and paraplegias. *Lancet*. 1983;1:1151-1155.
2. Klockgether T, Mariotti C, Paulson HL. Spinocerebellar ataxia. *Nat Rev Dis Primers*. 2019;5:24.
3. Taroni F, DiDonato S. Pathways to motor incoordination: The inherited ataxias. *Nat Rev Neurosci*. 2004;5:641-655.
4. Jacobi H, Reetz K, du Montcel ST, *et al*. Biological and clinical characteristics of individuals at risk for spinocerebellar ataxia types 1, 2, 3, and 6 in the longitudinal RISCA study: Analysis of baseline data. *Lancet Neurol*. 2013;12:650-658.
5. Velázquez-Pérez L, Rodríguez-Labrada R, Canales-Ochoa N, *et al*. Progression of early features of spinocerebellar ataxia type 2 in individuals at risk: A longitudinal study. *Lancet Neurol*. 2014;13:482-489.
6. Reetz K, Rodriguez-Labrada R, Dogan I, *et al*. Brain atrophy measures in preclinical and manifest spinocerebellar ataxia type 2. *Ann Clin Transl Neurol*. 2018;5:128-137.
7. Raposo M, Vasconcelos J, Bettencourt C, Kay T, Coutinho P, Lima M. Nystagmus as an early ocular alteration in Machado–Joseph disease (MJD/SCA3). *BMC Neurol*. 2014;14:17.
8. Oh AK, Jacobson KM, Jen JC, Baloh RW. Slowing of voluntary and involuntary saccades: An early sign in spinocerebellar ataxia type 7. *Ann Neurol*. 2001;49:801-804.
9. van Gaalen J, Maas RPPWM, Ippel EF, *et al*. Abnormal eyeblink conditioning is an early marker of cerebellar dysfunction in preclinical SCA3 mutation carriers. *Exp Brain Res*. 2019;237:427-433.
10. Serra HG, Duvick L, Zu T, *et al*. RORα-mediated Purkinje cell development determines disease severity in adult SCA1 mice. *Cell*. 2006;127:697-708.
11. Scoles DR, Meera P, Schneider MD, *et al*. Antisense oligonucleotide therapy for spinocerebellar ataxia type 2. *Nature*. 2017;544:362-366.
12. Rigo F, Hua Y, Krainer AR, Bennett CF. Antisense-based therapy for the treatment of spinal muscular atrophy. *J Cell Biol*. 2012;199:21-25.
13. Wood MJA, Talbot K, Bowerman M. Spinal muscular atrophy: Antisense oligonucleotide therapy opens the door to an integrated therapeutic landscape. *Hum Mol Genet*. 2017;26:R151-R159.
14. Koo T, Wood MJ. Clinical trials using antisense oligonucleotides in Duchenne muscular dystrophy. *Hum Gene Ther*. 2013;24:479-488.
15. Scaglioni D, Catapano F, Ellis M, *et al*. The administration of antisense oligonucleotide golodirsen reduces pathological regeneration in patients with Duchenne muscular dystrophy. *Acta Neuropathol Commun*. 2021;9:7.
16. Kasumu A, Bezprozvanny I. Deranged calcium signaling in Purkinje cells and pathogenesis in spinocerebellar ataxia 2 (SCA2) and other ataxias. *Cerebellum*. 2012;11:630-639.
17. Hekman KE, Gomez CM. The autosomal dominant spinocerebellar ataxias: Emerging mechanistic themes suggest pervasive Purkinje cell vulnerability. *J Neurol Neurosurg Psychiatry*. 2015;86:554-561.
18. Marr D. A theory of cerebellar cortex. *J Physiol*. 1969;202:437-470.
19. Albus JA. A theory of cerebellar function. *Math Biosci*. 1971;10:25-61.
20. Ito M, Itō M. *The cerebellum and neural control*. Raven Press; 1984.
21. Manto M, Bower JM, Conforto AB, *et al*. Consensus paper: Roles of the cerebellum in motor control—The diversity of ideas on cerebellar involvement in movement. *Cerebellum*. 2012;11:457-487.

22. Attwell PJE, Rahman S, Yeo CH. Acquisition of eyeblink conditioning is critically dependent on normal function in cerebellar cortical lobule HVI. *J Neurosci*. 2001;21:5715-5722.
23. Nguyen-Vu TDB, Kimpo RR, Rinaldi JM, *et al*. Cerebellar Purkinje cell activity drives motor learning. *Nat Neurosci*. 2013;16:1734-1736.
24. Schmahmann JD, Sherman JC. The cerebellar cognitive affective syndrome. *Brain*. 1998;121:561-579.
25. Parvizi J, Joseph J, Press DZ, Schmahmann JD. Pathological laughter and crying in patients with multiple system atrophy–cerebellar type. *Mov Disord*. 2007;22:798-803.
26. Chopra R, Bushart DD, Cooper JP, *et al*. Altered Capicua expression drives regional Purkinje neuron vulnerability through ion channel gene dysregulation in spinocerebellar ataxia type 1. *Hum Mol Genet*. 2020;29:3249-3265.
27. Robinson KJ, Watchon M, Laird AS. Aberrant cerebellar circuitry in the spinocerebellar ataxias. *Front Neurosci*. 2020; 14:707.
28. Lin X, Antalffy B, Kang D, Orr HT, Zoghbi HY. Polyglutamine expansion down-regulates specific neuronal genes before pathologic changes in SCA1. *Nat Neurosci*. 2000;3:157-163.
29. Serra HG, Byam CE, Lande JD, Tousey SK, Zoghbi HY, Orr HT. Gene profiling links SCA1 pathophysiology to glutamate signaling in Purkinje cells of transgenic mice. *Hum Mol Genet*. 2004;13:2535-2543.
30. Hoxha E, Balbo I, Miniaci MC, Tempia F. Purkinje cell signaling deficits in animal models of ataxia. *Front Synaptic Neurosci*. 2018;10:6.
31. Notartomaso S, Zappulla C, Biagioni F, *et al*. Pharmacological enhancement of mGlu1 metabotropic glutamate receptors causes a prolonged symptomatic benefit in a mouse model of spinocerebellar ataxia type 1. *Mol Brain*. 2013;6:48.
32. Smeets CJLM, Verbeek DS. Climbing fibers in spinocerebellar ataxia: A mechanism for the loss of motor control. *Neurobiol Dis*. 2016;88:96-106.
33. Paulson HL, Shakkottai VG, Clark HB, Orr HT. Polyglutamine spinocerebellar ataxias—From genes to potential treatments. *Nat Rev Neurosci*. 2017;18:613-626.
34. Burright EN, Brent Clark H, Servadio A, *et al*. SCA1 transgenic mice: A model for neurodegeneration caused by an expanded CAG trinucleotide repeat. *Cell*. 1995;82:937-948.
35. Clark HB, Burright EN, Yunis WS, *et al*. Purkinje cell expression of a mutant allele of SCA1 in transgenic mice leads to disparate effects on motor behaviors, followed by a progressive cerebellar dysfunction and histological alterations. *J Neurosci*. 1997;17:7385-7395.
36. Watase K, Weeber EJ, Xu B, *et al*. A long CAG repeat in the mouse Sca1 locus replicates SCA1 features and reveals the impact of protein solubility on selective neurodegeneration. *Neuron*. 2002;34:905-919.
37. Hourez R, Servais L, Orduz D, *et al*. Aminopyridines correct early dysfunction and delay neurodegeneration in a mouse model of spinocerebellar ataxia type 1. *J Neurosci*. 2011;31: 11795-11807.
38. Vig PJS, Wei J, Shao Q, Lopez ME, Halperin R, Gerber J. Suppression of calbindin-D28k expression exacerbates SCA1 phenotype in a disease mouse model. *Cerebellum*. 2012;11: 718-732.
39. Ruegsegger C, Stucki DM, Steiner S, *et al*. Impaired mTORC1-dependent expression of homer-3 influences SCA1 pathophysiology. *Neuron*. 2016;89:129-146.
40. Rousseaux MWC, Tschumperlin T, Lu HC, *et al*. ATXN1–CIC complex is the primary driver of cerebellar pathology in spinocerebellar ataxia type 1 through a gain-of-function mechanism. *Neuron*. 2018;97:1235-1243.e5.
41. Percie du Sert N, Hurst V, Ahluwalia A, *et al*. The ARRIVE guidelines 2.0: Updated guidelines for reporting animal research. *Br J Pharmacol*. 2020;177:3617-3624.
42. Titley HK, Watkins GV, Lin C, *et al*. Intrinsic excitability increase in cerebellar Purkinje cells after delay eye-blink conditioning in mice. *J Neurosci*. 2020;40:2038-2046.
43. Grasselli G, Boele HJ, Titley HK, *et al*. SK2 Channels in cerebellar Purkinje cells contribute to excitability modulation in motor-learning-specific memory traces. *PLoS Biol*. 2020;18: e3000596.
44. Schonewille M, Belmeguenai A, Koekkoek SK, *et al*. Purkinje cell-specific knockout of the protein phosphatase PP2B impairs potentiation and cerebellar motor learning. *Neuron*. 2010;67:618-628.
45. Beekhof GC, Osorio C, White JJ, *et al*. Differential spatiotemporal development of Purkinje cell populations and cerebellum-dependent sensorimotor behaviors. *Elife*. 2021:10: e63668.
46. Boele HJ, Peter S, Ten Brinke MM, *et al*. Impact of parallel fiber to Purkinje cell long-term depression is unmasked in absence of inhibitory input. *Sci Adv*. 2018;4:eaas9426.
47. White JJ, Bosman LWJ, Blot FGC, *et al*. Region-specific preservation of Purkinje cell morphology and motor behavior in the ATXN1[82Q] mouse model of spinocerebellar ataxia 1. *Brain Pathol*. 2021;31:e12946.
48. Ferreira TA, Blackman AV, Oyrer J, *et al*. Neuronal morphometry directly from bitmap images. *Nat Methods*. 2014;11:982-984.
49. Hansen ST, Meera P, Otis TS, Pulst SM. Changes in Purkinje cell firing and gene expression precede behavioral pathology in a mouse model of SCA2. *Hum Mol Genet*. 2013;22:271-283.
50. Cook AA, Fields E, Watt AJ. Losing the beat: Contribution of Purkinje cell firing dysfunction to disease, and its reversal. *Neuroscience*. 2021;462:247-261.
51. McCormick DA, Thompson RF. Neuronal responses of the rabbit cerebellum during acquisition and performance of a classically conditioned nictitating membrane–eyelid response. *J Neurosci*. 1984;4:2811-2822.
52. Thompson RF, Steinmetz JE. The role of the cerebellum in classical conditioning of discrete behavioral responses. *Neuroscience*. 2009;162:732-755.
53. Boele HJ, Koekkoek SK, De Zeeuw CI. Cerebellar and extracerebellar involvement in mouse eyeblink conditioning: The ACDC model. *Front Cell Neurosci*. 2010;3:19.
54. Miles FA, Lisberger SG. Plasticity in the vestibulo-ocular reflex: A new hypothesis. *Annu Rev Neurosci*. 1981;4:273-299.
55. Collewijn H. Eye- and head movements in freely moving rabbits. *J Physiol*. 1977;266:471-498.
56. Ito M. Cerebellar control of the vestibulo-ocular reflex—Around the flocculus hypothesis. *Annu Rev Neurosci*. 1982;5: 275-296.
57. Nagao S. Behavior of floccular Purkinje cells correlated with adaptation of vestibulo-ocular reflex in pigmented rabbits. *Exp Brain Res*. 1989;77:531-540.
58. Wulff P, Schonewille M, Renzi M, *et al*. Synaptic inhibition of Purkinje cells mediates consolidation of vestibulo-cerebellar motor learning. *Nat Neurosci*. 2009;12:1042-1049.
59. Louis ED, Kerridge CA, Chatterjee D, *et al*. Contextualizing the pathology in the essential tremor cerebellar cortex: A patholog-omics approach. *Acta Neuropathol*. 2019;138:859-876.
60. Kuo SH, Lin CY, Wang J, *et al*. Climbing fiber–Purkinje cell synaptic pathology in tremor and cerebellar degenerative diseases. *Acta Neuropathol*. 2017;133:121-138.
61. Barnes JA, Ebner BA, Duvick LA, *et al*. Abnormalities in the climbing fiber–Purkinje cell circuitry contribute to neuronal

dysfunction in ATXN1[82Q] mice. *J Neurosci*. 2011;31:12778-12789.
62. Duvick L, Barnes J, Ebner B, *et al*. SCA1-like disease in mice expressing wild-type ataxin-1 with a serine to aspartic acid replacement at residue 776. *Neuron*. 2010;67:929-935.
63. Ebner BA, Ingram MA, Barnes JA, *et al*. Purkinje cell ataxin-1 modulates climbing fiber synaptic input in developing and adult mouse cerebellum. *J Neurosci*. 2013;33:5806-5820.
64. Kuo PH, Gan SR, Wang J, *et al*. Dystonia and ataxia progression in spinocerebellar ataxias. *Parkinsonism Relat Disord*. 2017;45:75-80.
65. Mostofi A, Holtzman T, Grout AS, Yeo CH, Edgley SA. Electrophysiological localization of eyeblink-related microzones in rabbit cerebellar cortex. *J Neurosci*. 2010;30:8920-8934.
66. Thurling M, Kahl F, Maderwald S, *et al*. Cerebellar cortex and cerebellar nuclei are concomitantly activated during eyeblink conditioning: A 7 T fMRI study in humans. *J Neurosci*. 2015;35:1228-1239.
67. Otis TS, Kavanaugh MP, Jahr CE. Postsynaptic glutamate transport at the climbing fiber–Purkinje cell synapse. *Science*. 1997;277:1515-1518.
68. Hansel C, Linden DJ. Long-term depression of the cerebellar climbing fiber–Purkinje neuron synapse. *Neuron*. 2000;26:473-482.
69. Beeson KA, Beeson R, Westbrook GL, Schnell E. α2δ-2 Protein controls structure and function at the cerebellar climbing fiber synapse. *J Neurosci*. 2020;40:2403-2415.
70. Kano M, Hashimoto K, Chen C, *et al*. Impaired synapse elimination during cerebellar development in PKCγ mutant mice. *Cell*. 1995;83:1223-1231.
71. Kano M, Hashimoto K, Kurihara H, *et al*. Persistent multiple climbing fiber innervation of cerebellar Purkinje cells in mice lacking mGluR1. *Neuron*. 1997;18:71-79.
72. Ichikawa R, Hashimoto K, Miyazaki T, *et al*. Territories of heterologous inputs onto Purkinje cell dendrites are segregated by mGluR1-dependent parallel fiber synapse elimination. *Proc Natl Acad Sci U S A*. 2016;113:2282-2287.
73. Ichise T, Kano M, Hashimoto K, *et al*. Mglur1 in cerebellar Purkinje cells essential for long-term depression, synapse elimination, and motor coordination. *Science*. 2000;288:1832-1835.
74. Shuvaev AN, Horiuchi H, Seki T, *et al*. Mutant PKCγ in spinocerebellar ataxia type 14 disrupts synapse elimination and long-term depression in Purkinje cells *in vivo*. *J Neurosci*. 2011;31:14324-14334.
75. Becker EBE. The moonwalker mouse: New insights into TRPC3 function, cerebellar development, and ataxia. *Cerebellum*. 2014;13:628-636.
76. Konno A, Shuvaev AN, Miyake N, *et al*. Mutant ataxin-3 with an abnormally expanded polyglutamine chain disrupts dendritic development and metabotropic glutamate receptor signaling in mouse cerebellar Purkinje cells. *Cerebellum*. 2014;13:29-41.
77. Armbrust KR, Wang X, Hathorn TJ, *et al*. Mutant β-III spectrin causes mGluR1α mislocalization and functional deficits in a mouse model of spinocerebellar ataxia type 5. *J Neurosci*. 2014;34:9891-9904.
78. Titley HK, Brunel N, Hansel C. Toward a neurocentric view of learning. *Neuron*. 2017;95:19-32.
79. Schreurs BG, Gusev PA, Tomsic D, Alkon DL, Shi T. Intracellular correlates of acquisition and long-term memory of classical conditioning in Purkinje cell dendrites in slices of rabbit cerebellar lobule HVI. *J Neurosci*. 1998;18:5498-5507.
80. Belmeguenai A, Hosy E, Bengtsson F, *et al*. Intrinsic plasticity complements long-term potentiation in parallel fiber input gain control in cerebellar Purkinje cells. *J Neurosci*. 2010;30:13630-13643.
81. Lam YC, Bowman AB, Jafar-Nejad P, *et al*. ATAXIN-1 interacts with the repressor Capicua in its native complex to cause SCA1 neuropathology. *Cell*. 2006;127:1335-1347.
82. Berridge MJ, Irvine RF. Inositol trisphosphate, a novel second messenger in cellular signal transduction. *Nature*. 1984;312:315-321.
83. Walter JT, Alvina K, Womack MD, Chevez C, Khodakhah K. Decreases in the precision of Purkinje cell pacemaking cause cerebellar dysfunction and ataxia. *Nat Neurosci*. 2006;9:389-397.
84. Empson RM, Turner PR, Nagaraja RY, Beesley PW, Knöpfel T. Reduced expression of the Ca(2+) transporter protein PMCA2 slows Ca(2+) dynamics in mouse cerebellar Purkinje neurones and alters the precision of motor coordination. *J Physiol*. 2010;588:907-922.
85. Wu B, Blot FG, Wong AB, *et al*. TRPC3 Is a major contributor to functional heterogeneity of cerebellar Purkinje cells. *Elife*. 2019;8:e45590.
86. Inoue T, Lin X, Kohlmeier KA, Orr HT, Zoghbi HY, Ross WN. Calcium dynamics and electrophysiological properties of cerebellar Purkinje cells in SCA1 transgenic mice. *J Neurophysiol*. 2001;85:1750-1760.
87. Chopra R, Bushart DD, Shakkottai VG. Dendritic potassium channel dysfunction may contribute to dendrite degeneration in spinocerebellar ataxia type 1. *PLoS One*. 2018;13:e0198040.
88. Conquet F, Bashir ZI, Davies CH, *et al*. Motor deficit and impairment of synaptic plasticity in mice lacking mGluR1. *Nature*. 1994;372:237-243.
89. Gatchel JR, Watase K, Thaller C, *et al*. The insulin-like growth factor pathway is altered in spinocerebellar ataxia type 1 and type 7. *Proc Natl Acad Sci U S A*. 2008;105:1291-1296.
90. Kim JJ, Thompson RF. Cerebellar circuits and synaptic mechanisms involved in classical eyeblink conditioning. *Trends Neurosci*. 1997;20:177-181.
91. De Zeeuw CI, Hoebeek FE, Bosman LW, Schonewille M, Witter L, Koekkoek SK. Spatiotemporal firing patterns in the cerebellum. *Nat Rev Neurosci*. 2011;12:327-344.
92. Gerwig M, Hajjar K, Dimitrova A, *et al*. Timing of conditioned eyeblink responses is impaired in cerebellar patients. *J Neurosci*. 2005;25:3919-3931.
93. Timmann D, Gerwig M, Frings M, Maschke M, Kolb FP. Eyeblink conditioning in patients with hereditary ataxia: A one-year follow-up study. *Exp Brain Res*. 2005;162:332-345.
94. Gerwig M, Kolb FP, Timmann D. The involvement of the human cerebellum in eyeblink conditioning. *Cerebellum*. 2007;6:38-57.
95. Kronenbuerger M, Gerwig M, Brol B, Block F, Timmann D. Eyeblink conditioning is impaired in subjects with essential tremor. *Brain*. 2007;130:1538-1551.
96. Kashiwabuchi N, Ikeda K, Araki K, *et al*. Impairment of motor coordination, Purkinje cell synapse formation, and cerebellar long-term depression in GluRδ2 mutant mice. *Cell*. 1995;81:245-252.
97. Hansel C, Linden DJ, D'Angelo E. Beyond parallel fiber LTD: The diversity of synaptic and non-synaptic plasticity in the cerebellum. *Nat Neurosci*. 2001;4:467-475.
98. Schreurs BG. Changes in cerebellar intrinsic neuronal excitability and synaptic plasticity result from eyeblink conditioning. *Neurobiol Learn Mem*. 2019;166:107094.
99. van Beugen BJ, Gao ZY, Boele HJ, Hoebeek F, De Zeeuw CI. High frequency burst firing of granule cells ensures transmission at the parallel fiber to Purkinje cell synapse at the cost of temporal coding. *Front Neural Circuit*. 2013;7:95.

100. Schreurs BG, Tomsic D, Gusev PA, Alkon DL. Dendritic excitability microzones and occluded long-term depression after classical conditioning of the rabbit's nictitating membrane response. *J Neurophysiol*. 1997;77:86-92.
101. Cingolani LA, Gymnopoulos M, Boccaccio A, Stocker M, Pedarzani P. Developmental regulation of small-conductance $Ca^{2+}$–activated $K^+$ channel expression and function in rat Purkinje neurons. *J Neurosci*. 2002;22:4456-4467.
102. Hosy E, Piochon C, Teuling E, Rinaldo L, Hansel C. SK2 Channel expression and function in cerebellar Purkinje cells. *J Physiol*. 2011;589:3433-3440.
103. Alvina K, Khodakhah K. KCa channels as therapeutic targets in episodic ataxia type-2. *J Neurosci*. 2010;30:7249-7257.
104. Kasumu AW, Hougaard C, Rode F, *et al*. Selective positive modulator of calcium-activated potassium channels exerts beneficial effects in a mouse model of spinocerebellar ataxia type 2. *Chem Biol*. 2012;19:1340-1353.
105. Eteplirsen (Exondys 51) for Duchenne muscular dystrophy. *Med Lett Drugs Ther*. 2016; 58:145-146.
106. Claborn MK, Stevens DL, Walker CK, Gildon BL. Nusinersen: A treatment for spinal muscular atrophy. *Ann Pharmacother*. 2019;53:61-69.